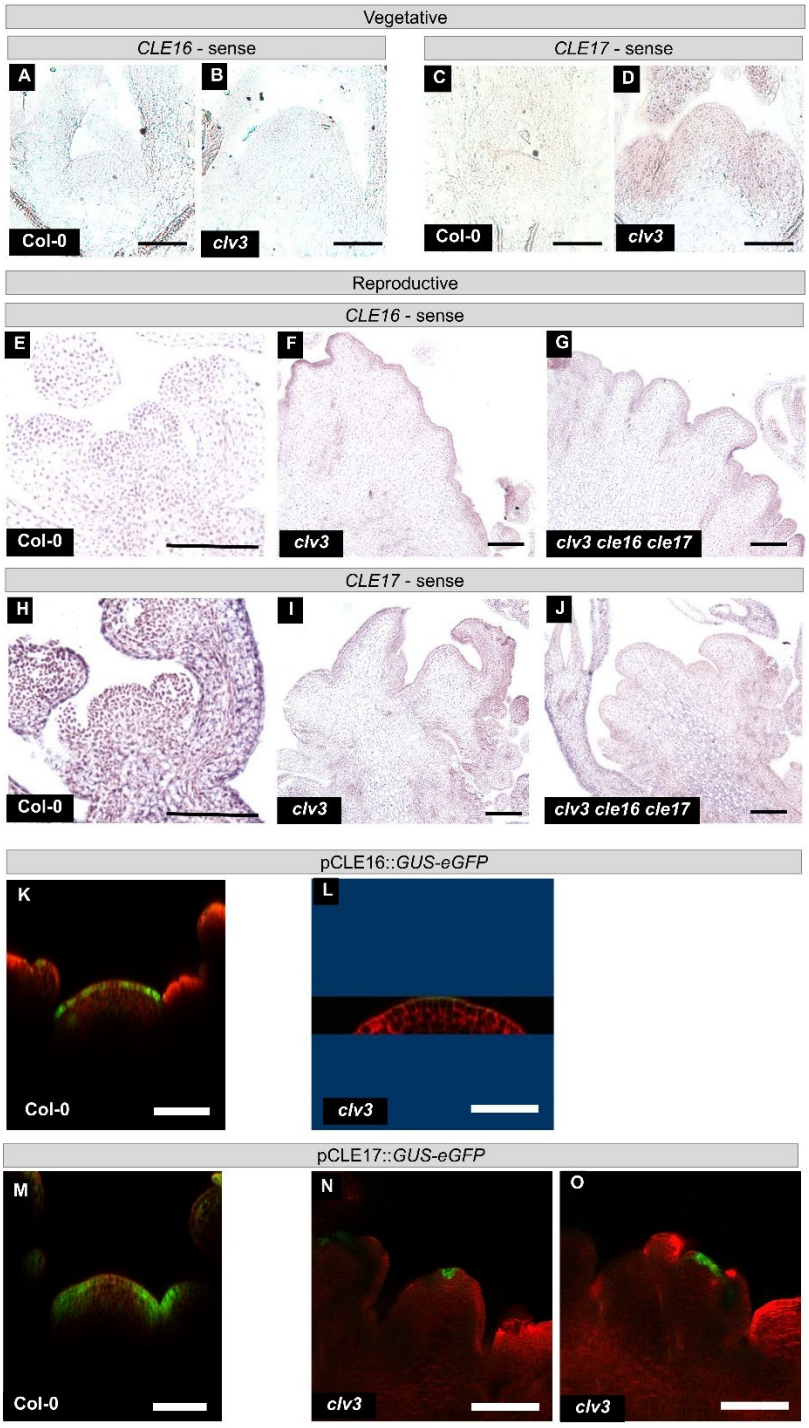

Fig. S1. CLE16 and CLE17 expression patterns in vegetative and reproductive shoot meristems, related to figure 1. A-D, Sense probe controls for mRNA *in situ* hybridization of *CLE16* (A, B) and *CLE17* (C, D) to 7 DAG vegetative SAMs of wild-type (A, C) and *clv3-15* (B, D) plants. E-J, Sense probe controls for mRNA *in situ* hybridization of *CLE16* (E-G) and *CLE17* (H-J) to IFMs of Col-0 (E, H), *clv3-15* (F, I) and *clv3 cle16 cle17* (G, J) plants. K-O, Confocal micrographs showing expression of pCLE16::GUS-eGFP (K, L) and pCLE17:GUS::eGFP (M-O) reporters in wild-type (K, M) and *clv3* (L, N, O) IFMs. Images in K, L, Mare reconstructed longitudinal sections from z-stacks. Images in N, O are single plane captures. Scale bars: 50 μm in A-D, 100 μm in E-O.

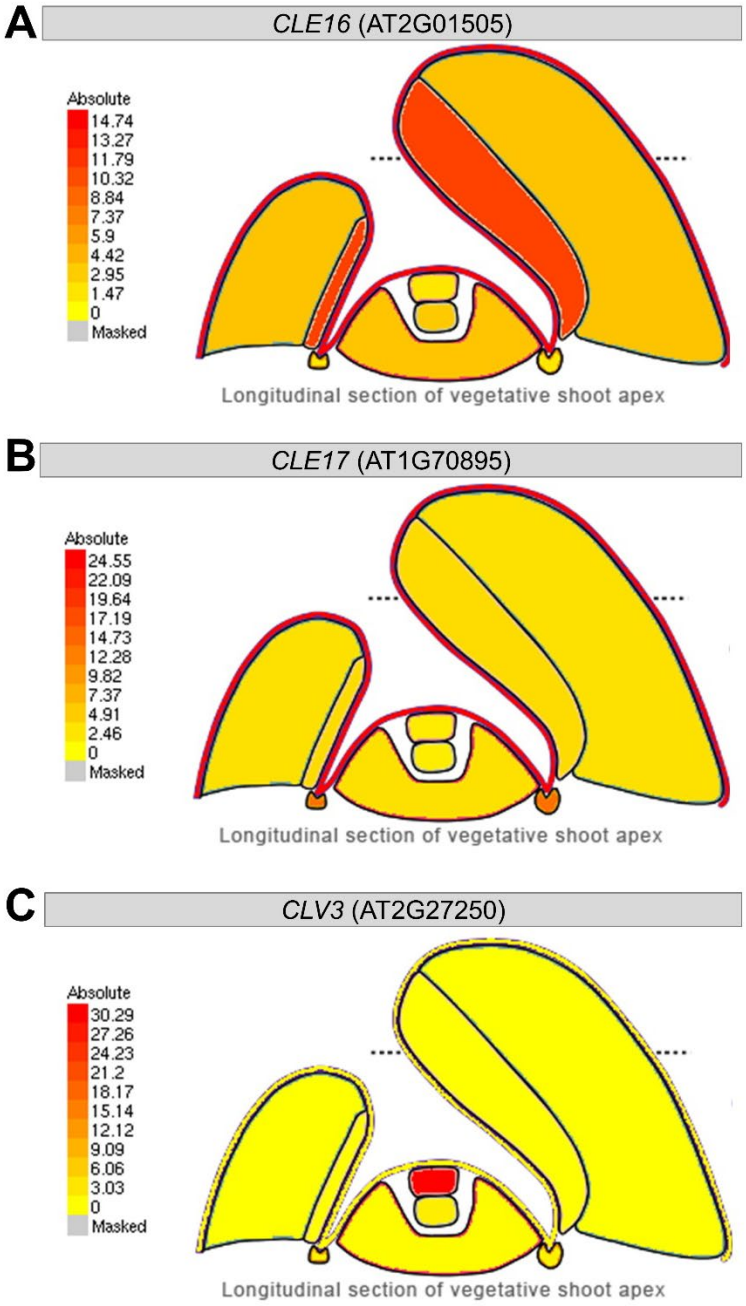

Fig. S2. eFP browser view of *CLE16, CLE17, CLV3,* and *ATML1* expression levels in Arabidopsis vegetative shoot meristems and leaf primordia, related to figure 1. *CLE16* (A), *CLE17* (B), and *CLV3* (C) normalized to RPKM units. An average of triplicates is shown. RNA-seq source data from Tian et al. (2014) and Tian et al. (2019).

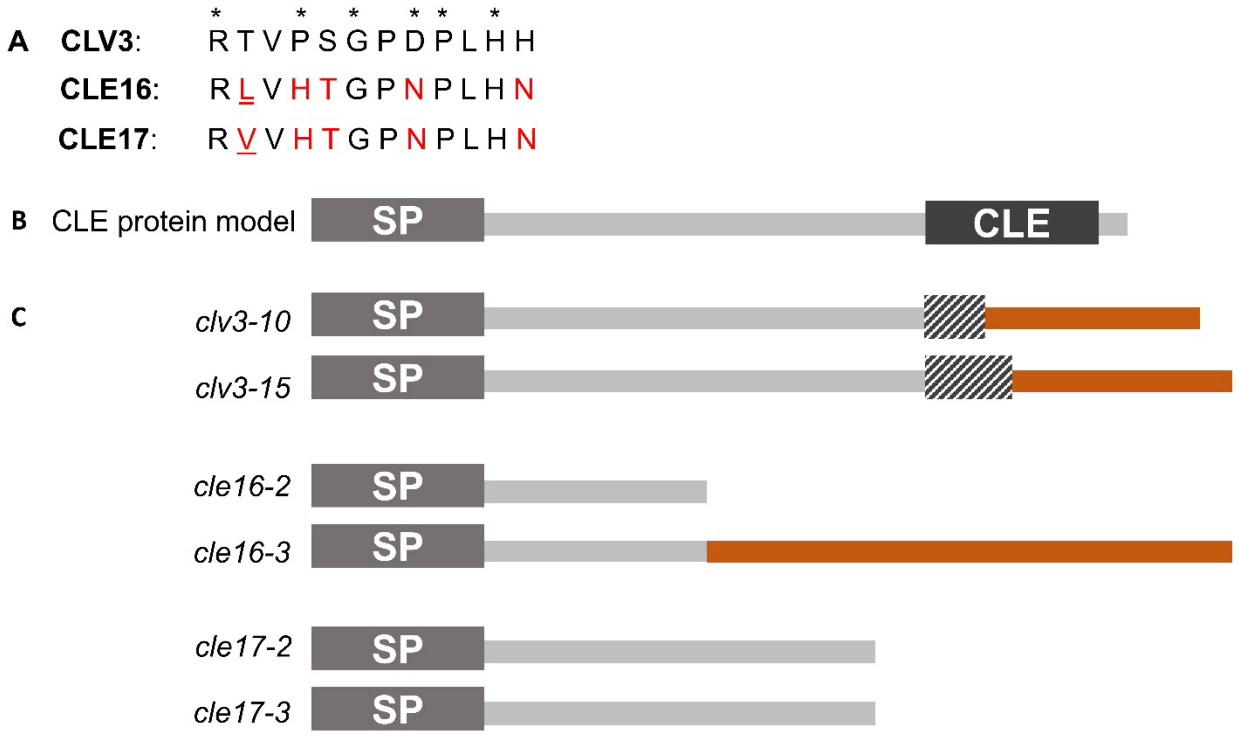

Fig. S3. CLE peptides and alleles used in this study. A, Alignment of the CLV3, CLE16, and CLE17 CLE domains. Asterisks denote amino acids in CLV3 that are important for receptor binding. Black text denotes amino acids that are conserved between all three proteins. B, Schematic of a generic CLE protein with an amino terminal signal peptide (SP), followed by a variable region and a 13 amino acid CLE domain. C, Schematics of mutant CLE pre-pro-peptides generated by the alleles used in this study. The *clv3-10* allele leads to a deletion and frameshift in the region encoding the CLV3 domain. The *clv3-15* allele leads to deletion of half of the CLV3 domain and its replacement with 36 random amino acids. The *cle16-3* allele leads to a frameshift upstream of the CLE domain. The *cle16-2*, *cle17-2* and *cle17-3* alleles each result in a premature stop codon upstream of the CLE domain. Hatched boxes denote deletions, and red lines denote random amino acid sequences induced by frameshifts in the mutant alleles.

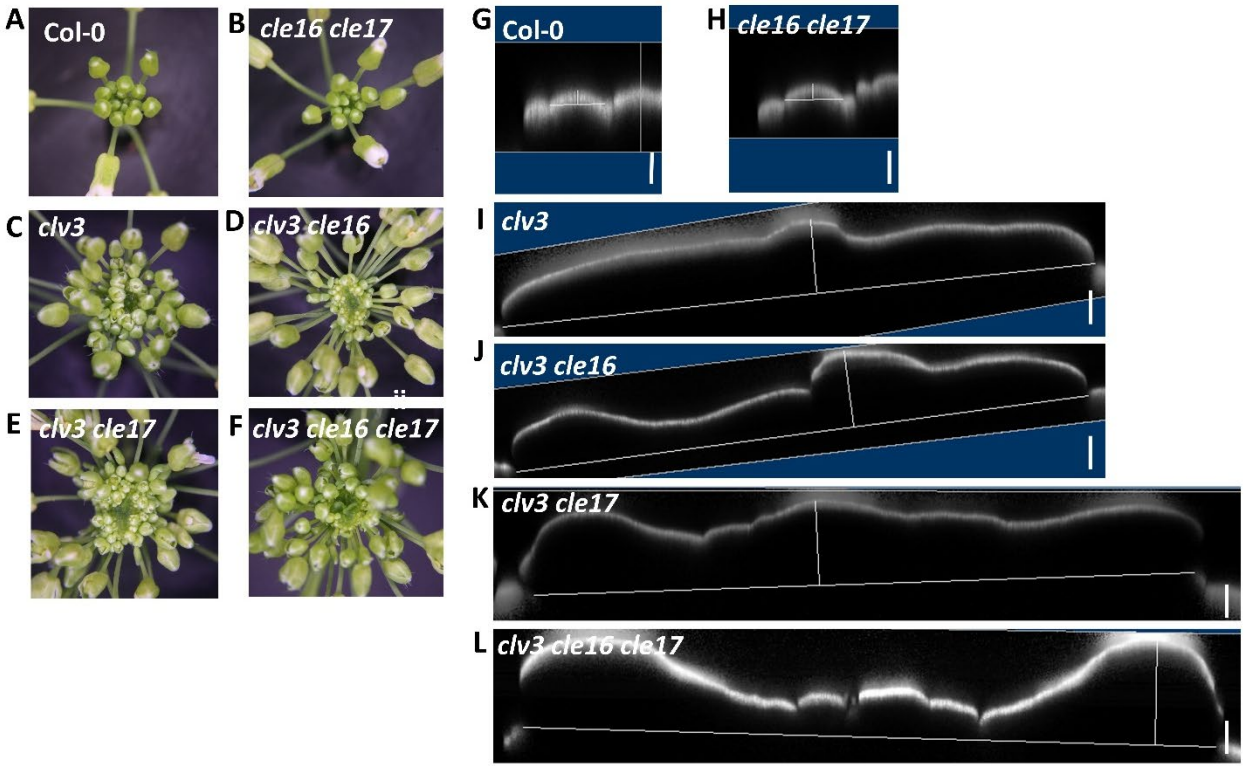

Fig. S4. *CLE16* and *CLE17* restrict stem cell accumulation in the inflorescence meristem in the absence of CLV3 activity, related to figure 2. Representative top-down view of inflorescences (A-F), and reconstructed longitudinal sections of inflorescence meristems from confocal stacks (G-L) from wild-type (A, G), *cle16 cle17* (B, H), *clv3* (C, I), *clv3 cle16* (D, J), *clv3 cle17* (E, K), and *clv3 cle16 cle17* (F, L) plants (n = 8 to 16). Scale bars: 300 µm.

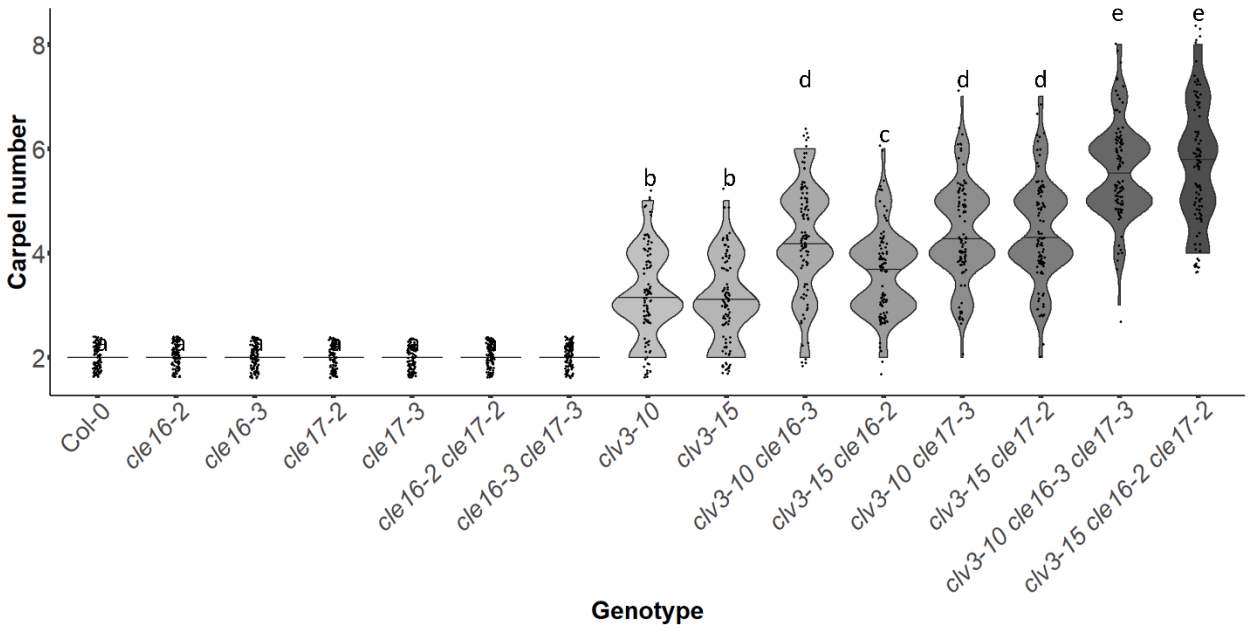

Fig. S5. Different combinations of *cle* alleles have the same effect on floral organ production, related to figure 3. Mean carpel number in wild-type, *cle16-2*, *cle16-3*, *cle17-2*, *cle17-3*, *cle16-2 cle17-2*, *cle16-3 cle17-3*, *clv3-10*, *clv3-15*, *clv3-10 cle16-3*, *clv3-15 cle16-2*, *clv3-10 cle17-3*, *clv3-15 cle17-2, clv3- 10 cle16-3 cle17-3* and *clv3-15 cle16-2 cle17-2* flowers (n = 100 flowers per genotype). Each dot in the violin plots represents the carpel number for an individual flower; and the middle line is the median. Statistical analysis was performed using one-way ANOVA and Tukey test; letters represent different significance groups at $P < 0.05$.

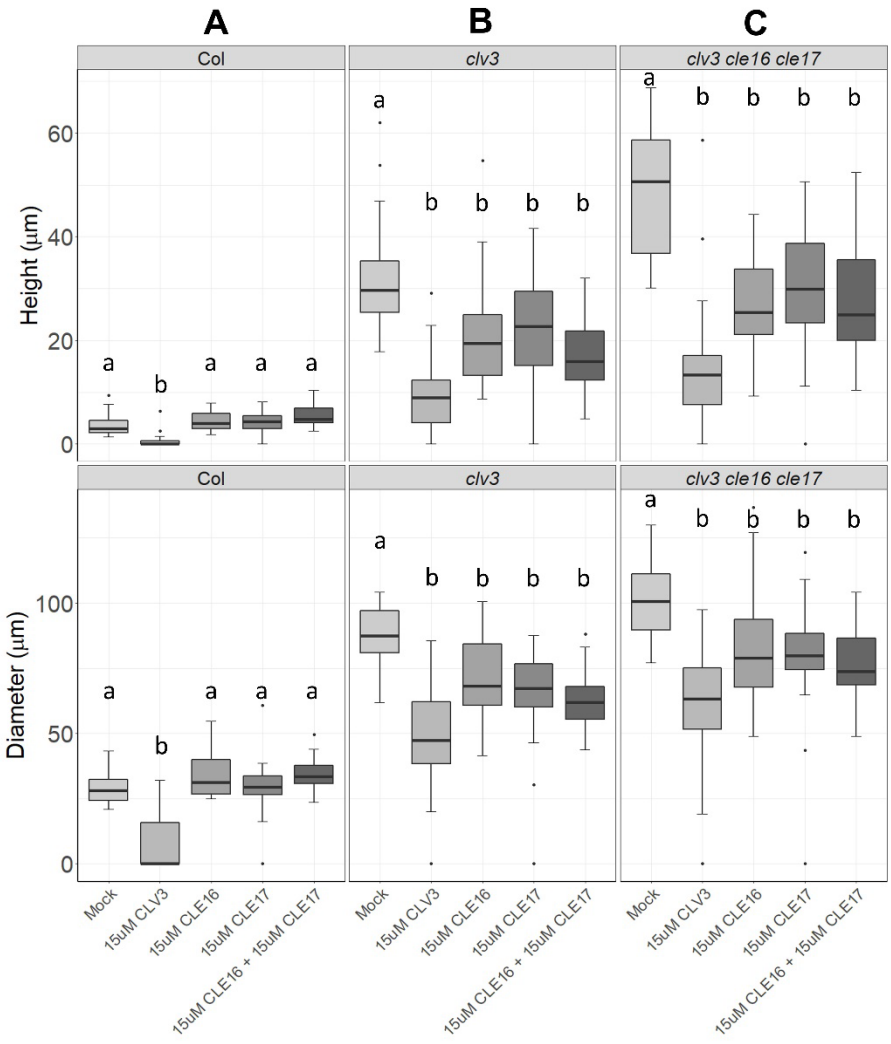

Fig. S6. CLE16 and CLE17 synthetic peptide treatments affect stem cell accumulation in the SAM in the absence of CLV3 activity, related to figure 4. Vegetative meristem size measurements of 7 DAG wild-type (A), *clv3* (B), and *clv3 cle16 cle17* (C) plants grown on MS plates containing a mock solution or 15 µM of synthetic CLV3, CLE16, CLE17, or CLE16 plus CLE17 peptide (n = 15 to 35). For the box plots, the bottom and top of the boxes represent the twenty-fifth and seventy-fifth percentile, respectively; the whiskers represent the minimum and maximum values; and the middle line is the median. Statistical analysis was performed using one-way ANOVA and Tukey test; letters represent different significance groups at $P < 0.05$.

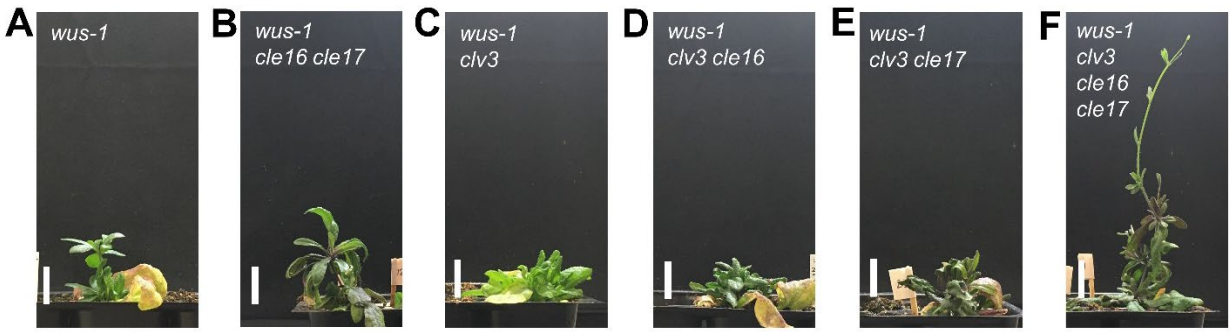

Fig. S7. Genetic interactions between *CLE16* and *CLE17* signaling pathways and *WUS*, related to figure 6. A-F, Side view of *wus-1* (A), *wus cle16 cle17* (B), *wus clv3* (C), *wus clv3 cle16* (D), *wus clv3 cle17* (E), and *wus clv3 cle16 cle17* (F) plants showing deficiency in shoot meristem maintenance. Scale bar: 2 cm.

Table S1. List of primers used in this study

Primer name	Sequence	Restriction enzyme
CLV3-F	ATGGATTCGAAGAGTTTTCTGCT	
CLV3-R	GACTCCCGAAATGGTAAAACCG	
CLE16-2-F	GAATCCAAAACCTGCTCTGC	MspI
CLE16-2-R	CGAAGGAGCAGTCAACACCT	
CLE17-2-F	ACTCCTCCGGAACAAGGTTT	BslI
CLE17-2-R	CTTCTGCACGCACTTTCTCA	